

Novel, High-Resolution, Subtractive Photoresist Formulations for 3D Direct Laser Writing Based on Cyclic Ketene Acetals

Marco Carlotti,* Omar Tricinci, and Virgilio Mattoli*

Direct laser writing (DLW) is an innovative technology based on two-photon polymerization processes which allow the 3D printing of architectures with arbitrary complexity at the (sub)micrometer scale. While most of the research interest in this field relies on additive manufacturing, subtractive approaches can be extremely helpful in nano/microfabrication, allowing the preparation of expendable scaffolds, replaceable parts, and for the protection of fragile structures. In this study, we show that the simple addition of 2-methylene-1,3-dioxepane, a cyclic ketene acetal compound, to a series of different acrylate-based photoresists results in functional formulations that allow the 3D-printing of degradable poly(ester-co-acrylate) microstructures via DLW. These latter could be degraded reliably under mild conditions compatible with other photoresists and materials of common use in the fabrication of MEMS, thus opening new opportunities to design novel fabrication procedures. In addition, the possibility of using different acrylate mixtures without affecting the degradability, allows the users to choose between a broad range of properties for the printed structures to fit their needs, without affecting the degradability. Finally, the authors show the potential of these photoresists in the fabrication of shadowing masks on 3D objects and their selective degradation employing a photobase.

technologies is advancing rapidly, pushing forward its limits in terms of new methodologies and materials.

In this scenario, 3D (sub)microprinting platforms are of particular interest as they allow the preparation of 3D micro and nano structures with high resolution and arbitrary complexity. One of the most up and coming technology in this regard is Direct Laser Writing (DLW),^[1,2] an additive manufacturing technique based on two-photon polymerization reactions which can be used to obtain (sub)micrometric objects and patterns with high throughput^[3] and a resolution below 100 nm.^[4] To achieve this, DLW makes use of a focused long-wavelength laser femto-second-pulse to irradiate a photosensitive resin able to crosslink under an energetic radiation.^[5] Although the absorption of the resin does not match the laser, in the focus the intensity of the radiation is high enough that multi-photon absorption phenomena may occur and initiate the polymerization process (or trigger decomposition for positive photoresist).


1. Introduction

There is little doubt that the technological revolution that we have experienced in the past two decades is intertwined with our ability to build smaller, smarter, faster, and more effective components and devices. Fueled by both fundamental and industrial interest, the research in micro- and nano- fabrication

As the resist is transparent to the laser, the printing only happens in a very small volume around the focus (the 'voxel', the 3D analogue of the 2D 'pixel'). By moving the latter around, one can obtain complex 3D architectures in one simple step. Because of its flexibility—together with the possibility to easily integrate functional materials—DLW has found several applications in MEMS,^[6] photonics,^[7] surface modification,^[8] security systems,^[9] and biomedical research.^[10,11]

The structures obtained with this technique are usually irreversible (being the result of extensive cross-link reactions), however, many applications would require the print of expendable scaffolds that aid the devices fabrication process and that one can remove when necessary. Such approaches take the name of subtractive manufacturing and consist in the fabrication of auxiliary structures with materials that can be removed, modified, or replaced on demand with simple, orthogonal procedures that do not affect the other printed parts.^[12] Such approach can offer solutions to print microstructures that are too fragile (or have geometric constraints) to be printed reliably, to develop functional devices with replaceable units,^[13] or even to protect fragile parts during subsequent fabrication steps. Furthermore, such materials could be useful for those applications which require the devices to

M. Carlotti, O. Tricinci, V. Mattoli
Center for Materials Interfaces
Istituto Italiano di Tecnologia
Viale Rinaldo Piaggio 34, Pontedera 56025, Italy
E-mail: marco.carlotti@iit.it; virgilio.mattoli@iit.it

 The ORCID identification number(s) for the author(s) of this article can be found under <https://doi.org/10.1002/admt.202101590>.

© 2022 The Authors. Advanced Materials Technologies published by Wiley-VCH GmbH. This is an open access article under the terms of the Creative Commons Attribution License, which permits use, distribution and reproduction in any medium, provided the original work is properly cited.

DOI: 10.1002/admt.202101590

degrade to perform their function such as carriers for biomedical applications and in disposable electronics. In addition, these technologies could work synergistically with other functional resists fabrication of functioning MEMS devices intrinsically capable of responding to external stimuli,^[14,15] sensing,^[16] show enhanced properties,^[17–19] controlled actuation,^[20,21] and shape recovery.^[22]

Few solutions were proposed recently to bring subtractive manufacturing to DLW. Oxygen plasma, for example, can effectively remove thin structures,^[13,23] but, by acting on the entirety of the structure, lacks sensitivity and thus requires optimization of the different printing parameters to obtain the desired design. In an early study, Adzima et al. showed that Diels–Alder networks can degrade upon thermal stimulations,^[24] although high temperatures are usually required. Researchers at the Karlsruhe Institute of Technology produced several studies comprising interesting chemical solutions^[25] by preparing materials that once polymerized could then be decomposed selectively and locally by chemical stimuli,^[26,27] interaction with light,^[28] water,^[29] or enzymes.^[30]

However, while the performances of these materials are remarkable, synthetic procedures which require the intervention of trained chemists are often an obstacle to the spreading of novel resins. This is particularly the case of printing manufacturing techniques which are used in disparate fields by people with diverse backgrounds and needs. Simple and affordable formulations for subtractive manufacturing based on commercially available products can therefore be useful in this sense, allowing the simple preparation of photoresists with reproducible and well understood properties.

With these premises in mind, we decided to investigate the use in 3D microfabrication of aliphatic polyesters. These polymers are a well known class of materials which combine degradability with mechanical robustness. Poly(lactic acid) (PLA), poly(glycolic acid) (PGA), and poly(caprolactone) (PCL)^[31] are all examples of commonly employed aliphatic polyesters with plenty of applications in diverse fields. Nevertheless, the most common synthetic procedures to prepare polyesters comprise polycondensation, transesterification, and ring opening polymerization reactions which make use of cationic, anionic, or metal catalyst, rendering them non-viable for our 3D microprinting scopes.

Cyclic ketene acetals (CKAs) offer a way to circumvent this obstacle.^[32–35] While most common monomers used in DLW are acrylates, which efficiently polymerize under the radical conditions employed to yield resilient and inert networks, radical ring opening polymerization of CKAs results instead in the formation of aliphatic polyesters analogues to the ring opening polymerization of lactones (**Figure 1**).^[36–39] The structures realized using these materials should therefore be inherently susceptible to degradation by bases, nucleophiles, and appropriate biological systems while still maintaining the good structural and mechanical properties typical of aliphatic polyesters and related copolymers.^[36,40–43]

In this paper, we report the use of 2-methylene-1,3-dioxepane (MDO), one of the most stable and readily available CKAs, as additive in commercial acrylate-based photoresists (such as IP-L) or in combination with common acrylate crosslinkers (such as pentaerythritol tetraacrylate, PETA, and polyethylene glycol diacrylate, PEG-DA) as novel photoresist formulations for the preparation of degradable poly(ester-co-acrylate)

microstructures via DLW (**Figure 1**). We show that such structures could be degraded reliably under mild conditions compatible with other photoresists and materials of common use in the fabrication of MEMS, thus opening new opportunities to design novel fabrication procedures. The possibility of employing different co-monomers, without drastically affecting the degradation properties, can allow the user to prepare a formulation with the properties that better fit their needs. In addition, we also show that structures comprising polymerized MDO can even be locally degraded with the use of an appropriate photobase-solvent mixture which can operate upon two-photon absorption.

2. Results and Discussion

The radical ring opening polymerization of MDO results in the formation of polyesters analogues to PCL,^[44] thus allowing for the direct introduction of aliphatic ester moieties in the polymeric chains via DLW. The resulting microstructures should therefore possess mechanical robustness and be degradable in suitable conditions.

Preliminary polymerization experiments using an MDO:photoinitiator mixture did not yield any appreciable result using both two-photon and one-photon methodologies. Upon irradiation with a UV lamp, the as prepared resin grew more viscous but did not solidify. IR analysis (**Figure S1**, Supporting Information) showed a broad peak at $\approx 3300\text{ cm}^{-1}$ which can be ascribed to the presence of hydroxy groups, indicating a non-successful polymerization. Indeed, it was often reported that rROP of CKAs often leads to incorporation of defects due to non-optimal radical isomerization of the molecules.^[33,45,46] Such defects include incorporation of acetal groups due to an inefficient ring opening mechanism and ramifications arising from H abstractions.^[44] It is not surprising that in the peculiar conditions typical of two-photon lithography—involving high energies and uneven power distributions—MDO polymerization does not proceed as it would in a controlled environment.

Many studies, however, demonstrated the versatility of MDO in copolymerizing with diverse co-monomers, like acrylates and vinyls, to prepare degradable materials with variegated mechanical properties.^[36,40–42,47] We therefore prepared mixtures of MDO with several acrylates which could function as crosslinker. Initially, we tested formulations comprising PETA, a tetra functional acrylate, and MDO. We found that 5 wt% of PETA (in presence of 5 wt% Omnirad 379 as photoinitiator) was sufficient to produce the desired result. **Figure 2** shows some of the structures we prepared using the aforementioned formulation, highlighting how it can be used to prepare robust and tall structures like a micro Michelangelo's David and a micro Darth Vader with high-resolution.

To test the printing parameters of the photoresist, we printed a series of solid and woodpile structures (**Figure 2**). For the former, a power of $\approx 20\text{ mW}$ (40% of nominal 50 mW full power at the lens) and a scan speed of $7500\text{ }\mu\text{m s}^{-1}$ gave the best result. Above that threshold, structures could still be written but we observed a loss of definition as the voxel grew in size. Only increasing the power well above the previous limits resulted in micro explosions of the resist. Woodpiles required a higher radiant energy in order to produce self-standing structures

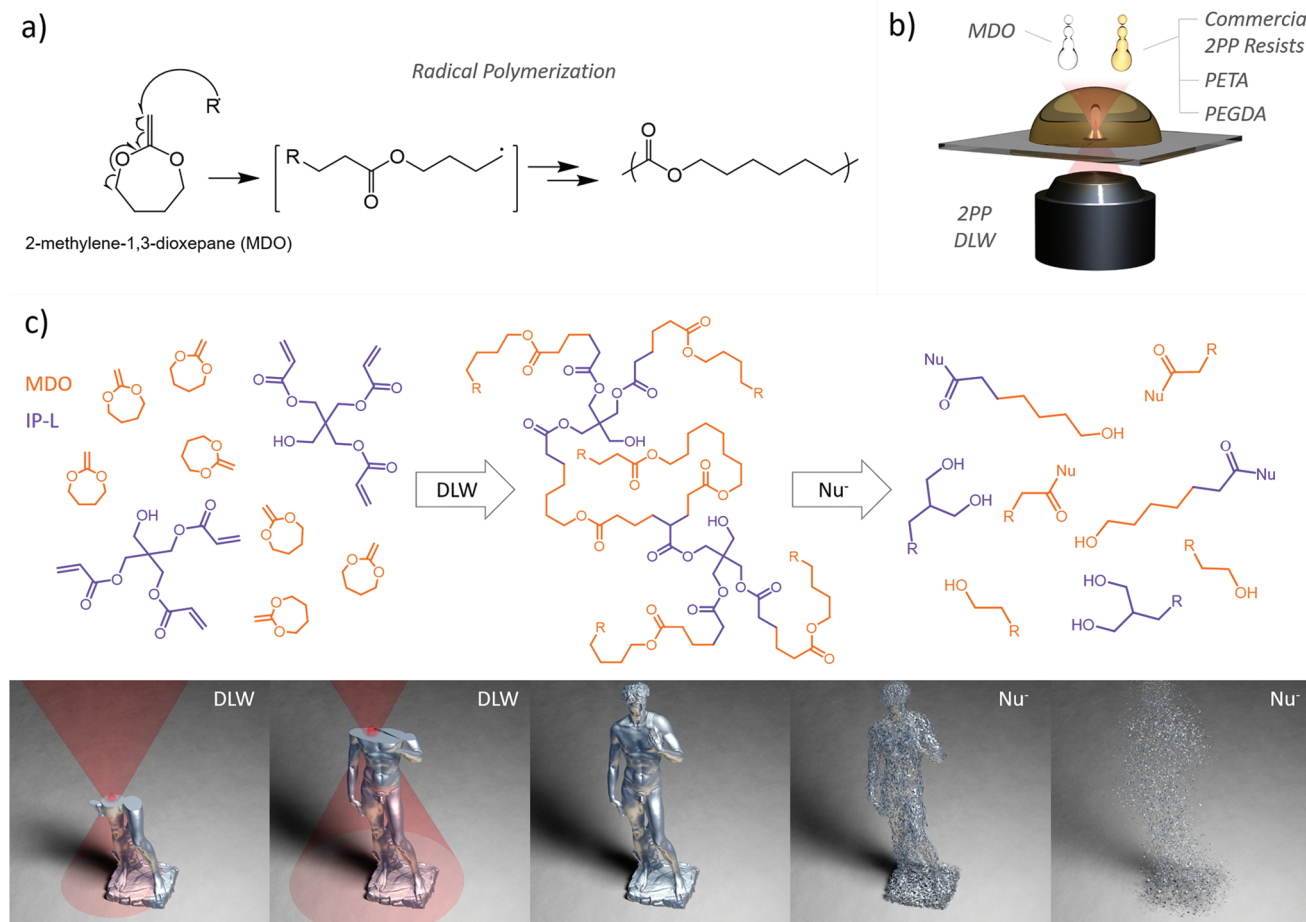


Figure 1. a) Radical ring opening polymerization mechanism of MDO yielding PCL. b) Sample preparation for the DLW process. MDO is incorporated in the photoresist formulation by simple mixing. c) Working principle of a photoresist comprising MDO: through the DLW process aliphatic polyester moieties are incorporated in the cross-linked network; upon treatment with a nucleophile (Nu⁻) these latter decompose, degrading the microstructure. The cleavage of ester bond through the action of a nucleophile happens between the carbonyl and the oxygen (not shown for clarity).

without deformation (for 20 mW of power we employed a scan speed of 2000 $\mu\text{m s}^{-1}$). In these, the linewidth was $\approx 1 \mu\text{m}$, which however is much larger than the smallest possible ($\approx 400 \text{ nm}$).

Addition of Cyrene as inert solvent up to 25 wt% did not compromise the writing process but, on the contrary, seemed to extend the optimal power range (Figures S5 and S6, Supporting Information). However, woodpiles obtained with this formulation looked more prone to shrinking compared to the previous examples, but were self-standing nevertheless.

The ester linkages in MDO-based materials are prone to the attack from nucleophiles,^[37–39,43] aqueous acids,^[42] and biomolecules^[34,40] (e.g., lipases) which can result in the shortening of the polymeric chains and the degradation of the structure. We therefore evaluated the degradability of DLW microstructures in several environments. We found that KOH in warm methanol (0.5 M) gave good results, dissolving structures in $\approx 2 \text{ h}$ (Figure 3). Residues that could be ascribed to the degradation of polyesters could be found in the digesting solution after the degradation process (see Supporting Information). Decreasing the concentration of the base or the temperature slows the degradation process, while an increment of these parameters

speeds the latter up (see Table 1 and Supporting Information). Aqueous solutions, both basic and acidic, seemed to be less effective (also, they often resulted in the detachment of the structures from the glass substrate). This observation could be related to the low affinity between water and the polymerized parts which prevents intimate contact between the structures and the solution. During the degradation process, a loss of definition of the structure anticipates the reduction in size as one would expect from the degradation mechanism of aliphatic polyesters. Notably, as we show in Figure 3, the degradation procedure does not affect commercial resists commonly employed in DLW, which can be used in tandem with MDO-based ones without the need of any precaution. This evidence also supports the hypothesis that MDO units have efficiently been incorporated in the resulting network. Although we could not measure directly the MDO fraction in the structures,^[48] we can still affirm that it is sufficient to trigger the degradation. These analyses are not easily performed on DLW-printed microstructures, especially to extract quantitative information. Considerations on the lower reactivity of CKAs compared to that of acrylates would suggest that the incorporated fraction is lower than that in the starting formulation.^[37,43,45]

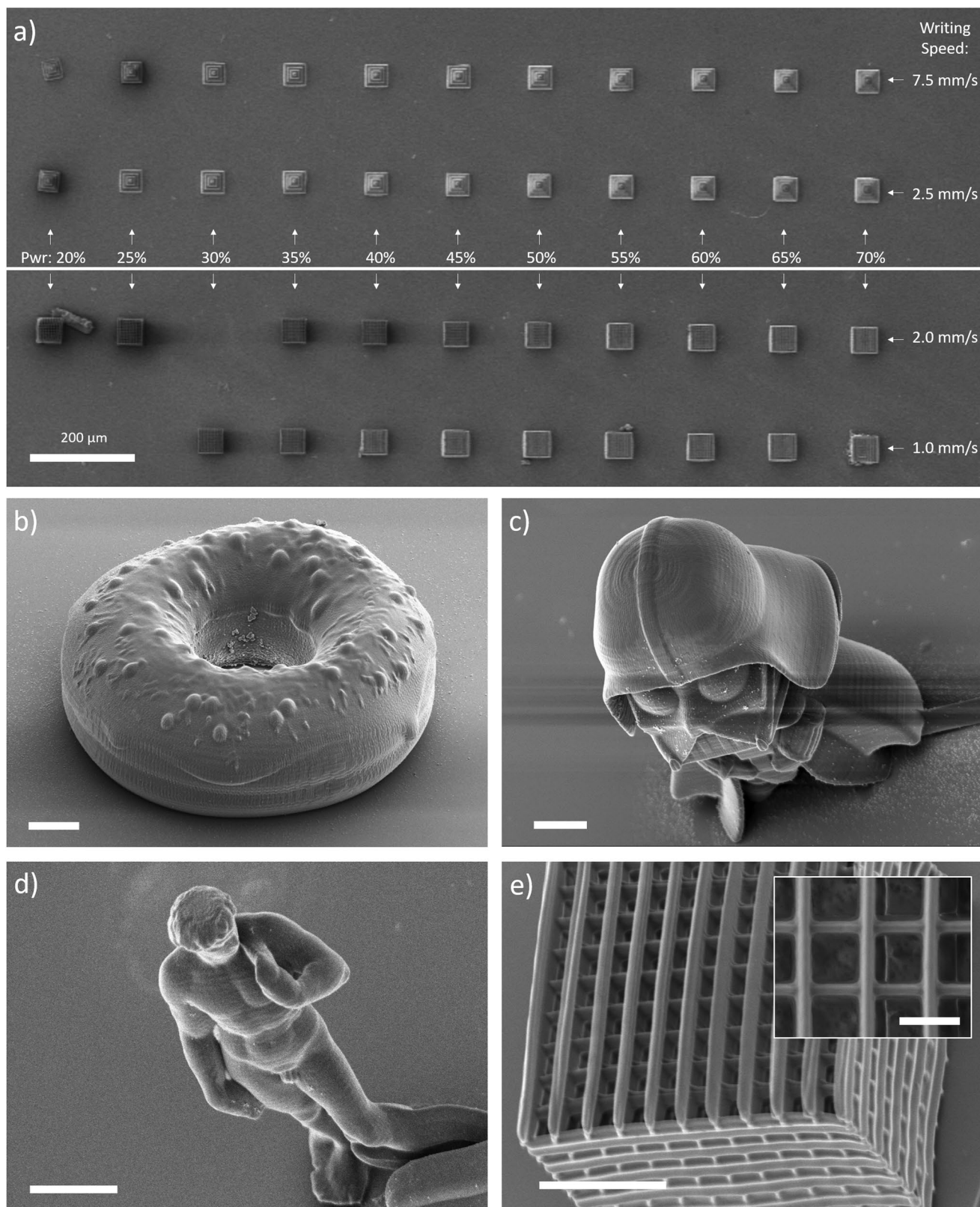


Figure 2. SEM pictures of example structures realized employing 90:10 MDO:PETA (+5 wt% Omnirad) formulation. a) Array of micro-pyramids and woodpiles realized with different laser powers and scan speeds. b) A micro-donut. c) A micro-DarthVader. d) A micro Michelangelo's David. e) A woodpile structure (laser power 60%, writing speed 2 mm s⁻¹ from panel (a)). Scale bars are 20 μm. Inset of panel (e) represent a magnification of same structure (scale bar 5 μm).

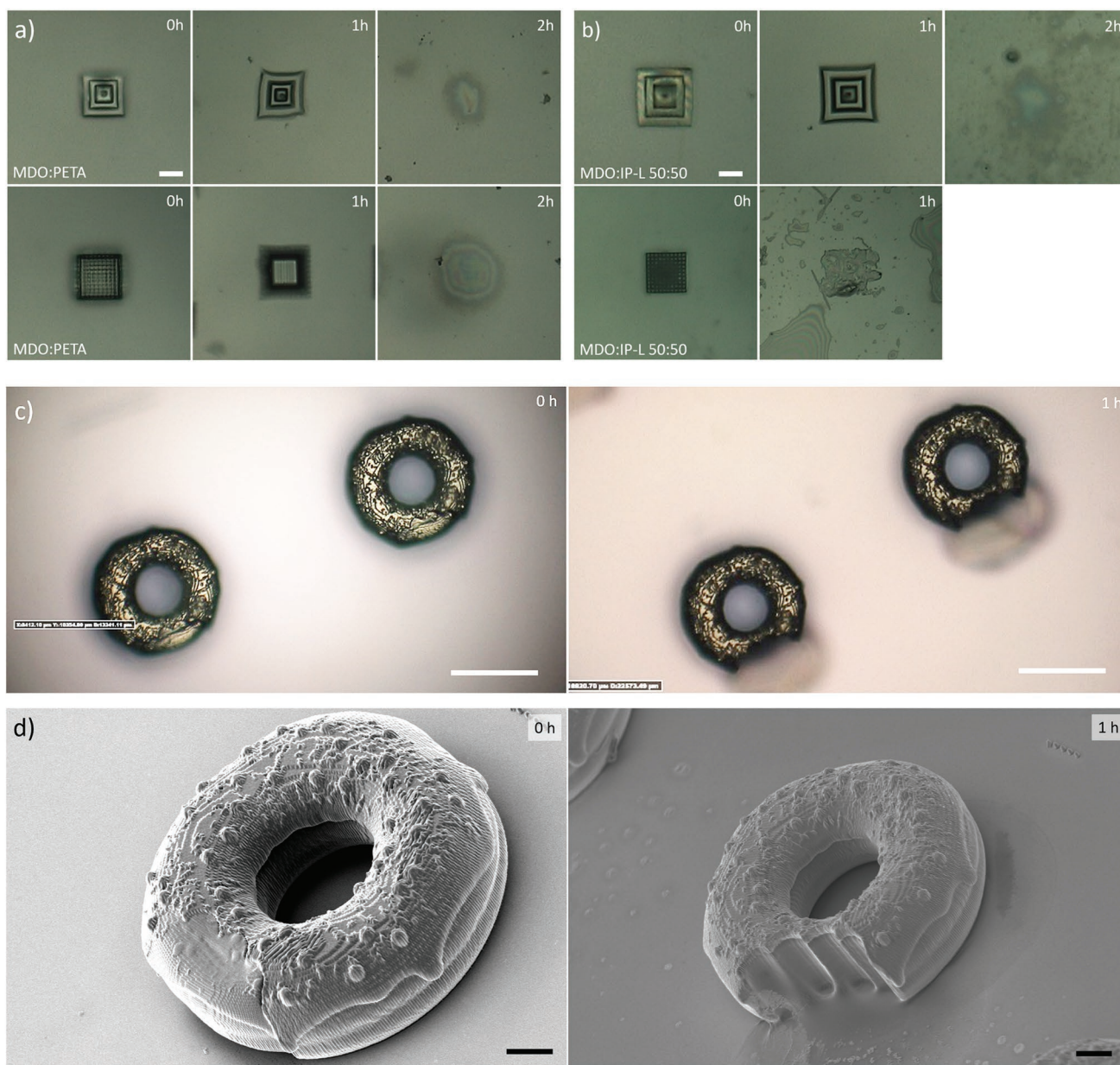


Figure 3. Examples of degradation of printed micro-structures comprising MDO. Optical microscopy pictures of degradation of pyramid and woodpile structures in KOH 0.5 M in MeOH at 50 °C realized using MDO:PETA 90:10 (a) and MDO:IP-L 50:50 (b). Scale bar 20 μm . c) Partial degradation of micro-donuts structures which were realized using IP-L and MDO:PETA 90:10 (scale bar 100 μm). Only the latter part degrades leaving out the bite mark. d) SEM pictures of the previous structures (scale bar 20 μm).

Employing more than 30 wt% PETA resulted in non-degradable structures even at low powers, indicating a high degree of crosslinking.

To show the versatility of CKAs as additives for the formulation of all-purpose photoresists and broaden their possible applications, we added MDO to the commercial resist IP-L. The latter is composed by pentaerythritol triacrylate and up to 5 wt% of photoinitiator. With one less acrylate functionality, we expect these formulations to be more flexible on the composition and the resulting properties. Indeed, formulations comprising an MDO:IP-L composition in the 1:3 to 3:1 range resulted in the printing of microstructures similar to those

discussed earlier, with the only difference that a higher power was needed, probably as a consequence of a lower amount of photoinitiator present in the mixture due to dilution (Figure S7, Supporting Information). The successful printing of structures with such diverse MDO:cross-linker ratio shows the versatility of the system we are proposing. The variation of the MDO:IP-L ratio affects the properties of the resist and the printing performances. As we show in the SEM images reported in Figure S7, Supporting Information, increasing the fraction of IP-L in the mixture resulted in more defined structures even at lower laser powers. We found these structures to have similar degradation properties to the aforementioned MDO:PETA ones (Figure 3).

Table 1. Summary of degradation tests of different formulations and degradation conditions.

Photoresist composition	Degradation conditions	Degradation time
MDO:PETA 90:10	KOH 0.5 M MeOH 50 °C	2 h
	KOH 2 M MeOH rt	20 h
	KOH 2 M MeOH 50 °C	1 h
	KOH 2.5 M water 70 °C	5 h
	H ₂ SO ₄ 25% 70 °C	8 h
MDO:PETA:Cyrene 90:10:25	KOH 0.5 M MeOH 50 °C	2 h
MDO:PETA 70:30	KOH 2 M MeOH 50 °C	4 h
MDO:IP-L 75:25	KOH 0.5 M MeOH 50 °C	0.5 h
MDO:IP-L 50:50	KOH 0.5 M MeOH 50 °C	1 h
	KOH 2.5 M water 70 °C	5 h
	AZ Remover 50 °C	8 h
	H ₂ SO ₄ 25% 70 °C	10 h
MDO:IP-L 25:75	KOH 0.5 M MeOH 50 °C	6 h
MDO:PEG-DA 20:80	KOH 0.5 M MeOH 50 °C	1 h
	H ₂ SO ₄ 25% 70 °C	8 h

This is particularly surprising in the case of IP-L, which can be employed both as an additive and subtractive manufacturing resist upon simple addition of MDO to the formulation without further precautions or processing.

Remarkably, the addition of MDO only affected to a small extent the mechanical properties of the microstructures. In particular, we measured the Young modulus (E) of a 1:3 MDO:IP-L composition to be 3.1 ± 0.4 GPa when printed using an energy radiance which resulted in an E of 4.3 ± 0.5 GPa for pure IP-L despite the lower amount of photoinitiator present. By increasing the energy radiance, E also increased in value and values comparable with those of pure IP-L were obtained even for formulation comprising 50% MDO (4.2 ± 0.6 GPa, see Supporting Information). This observation can be ascribed to the similar E measured for many polyesters and polyacrylates, however, MDO containing structures present a very different yield stress, hinting to their different chemical nature.

Next to tetra- and tri-functional acrylates, we also tested di-functional acrylates. We obtained reasonable results employing PEG-DA, a monomer commonly used in DLW for its biocompatibility, affinity to water, and its low Young modulus. We show the result of DLW employing an MDO:PEG-DA 2:8 (plus 5 wt% photoinitiator) formulation in Figure S7, Supporting Information. Compared to the formulations introduced so far, the latter is characterized by a much lower resolution, as it is common for photoresists employing PEG-DA.^[1] Remarkably, also in this case the printed parts could be selectively degraded using the same procedures, actually performing better in diluted aqueous acids (Table 1).

The use of a photoresist that can be easily and selectively removed can offer novel approaches for microfabrication. It can allow, for instance, the preparation of sacrificial masks analogous to what one can achieve with 2D lithography but on 3D objects. In this sense, one can employ the photoresist formulations introduced herein, in combination with other standard

nano/microfabrication procedures, for the fabrication of components and devices that cannot be easily realized with either DLW or 2,(5)D techniques alone. To show this potential, we printed a bridge using standard photoresist and patterned the sides and the top using a photoresist formulation comprising MDO in order to realize the negative of a serpentine. After sputtering of a gold layer, the subtractive resist was removed in 0.5 M KOH in methanol, leaving behind a well-defined Au path connecting the two halves of the bridge. SEM and Focused Ion Beam (FIB) photographs (Figure 4) showed that we were able to obtain defined regions with isolating properties on the bridge, no differently than what one would get from common lithographic techniques on a flat surface. We are currently working to implement this technology for the preparation of MEMS and components.

While the selective removal of a certain resist with a reagent can be useful for high-throughput fabrication, removal of selective parts of a 3D-structure comprising the same photoresist can unfold in unprecedented methodologies for micro-nanofabrication. Being aware of the limited stability of aliphatic polyesters toward nucleophiles, we decided to employ a solution of a photobase (4-amino-quinoline, 4AQ) in methanol which, upon excitation, can generate locally a high concentration of methoxide ions.^[49,50] The choice of 4AQ was tied to its strong absorption at ≈ 390 nm (i.e. so to allow two-photon absorption with our DLW setup) and to its ability to deprotonate methanol in the excited state.^[51] Remarkably, by using a laser power and scan speeds which we also employed during the earlier writing step (15 mW and a scan speed of $5000 \mu\text{m s}^{-1}$), we could achieve a precise and selective removal of the resist. Figure 4 highlights few details of these operations and the possible resulting geometries. Studies are currently underway to evaluate if we can apply the same methodology to other common photoresists formulations.

3. Conclusions

In conclusion, in this study we demonstrated how it is possible to reliably obtain subtractive manufacturing resist formulations for DLW simply employing CKAs in combination with common (tetra-, tri-, and di-functional) acrylate crosslinkers or commercial acrylate-based resists such as the IP series. The use of compounds such as MDO during the radical DLW printing process, allows for the insertion of aliphatic esters in the polymerized chains, which are prone to degradation mediated by nucleophiles. In addition, these materials are commercially available, without requiring any synthetic efforts.

The printed microstructures are stable, mechanically reliable, and are characterized by high resolutions which depend on the acrylate co-monomer(s) used. Upon exposition to basic or acidic environments (or other agents capable of breaking up aliphatic esters) one can degrade the printed structures rapidly and on demand. This can allow the users to design simple and effective procedures to take advantage of erasable scaffolds, substitutions of parts, protective coatings, and 3D sacrificial masks. The possibility of using several acrylate co-monomers, characterized by the different nature and number of polymerizing groups, allow the potential users to transfer the degradability

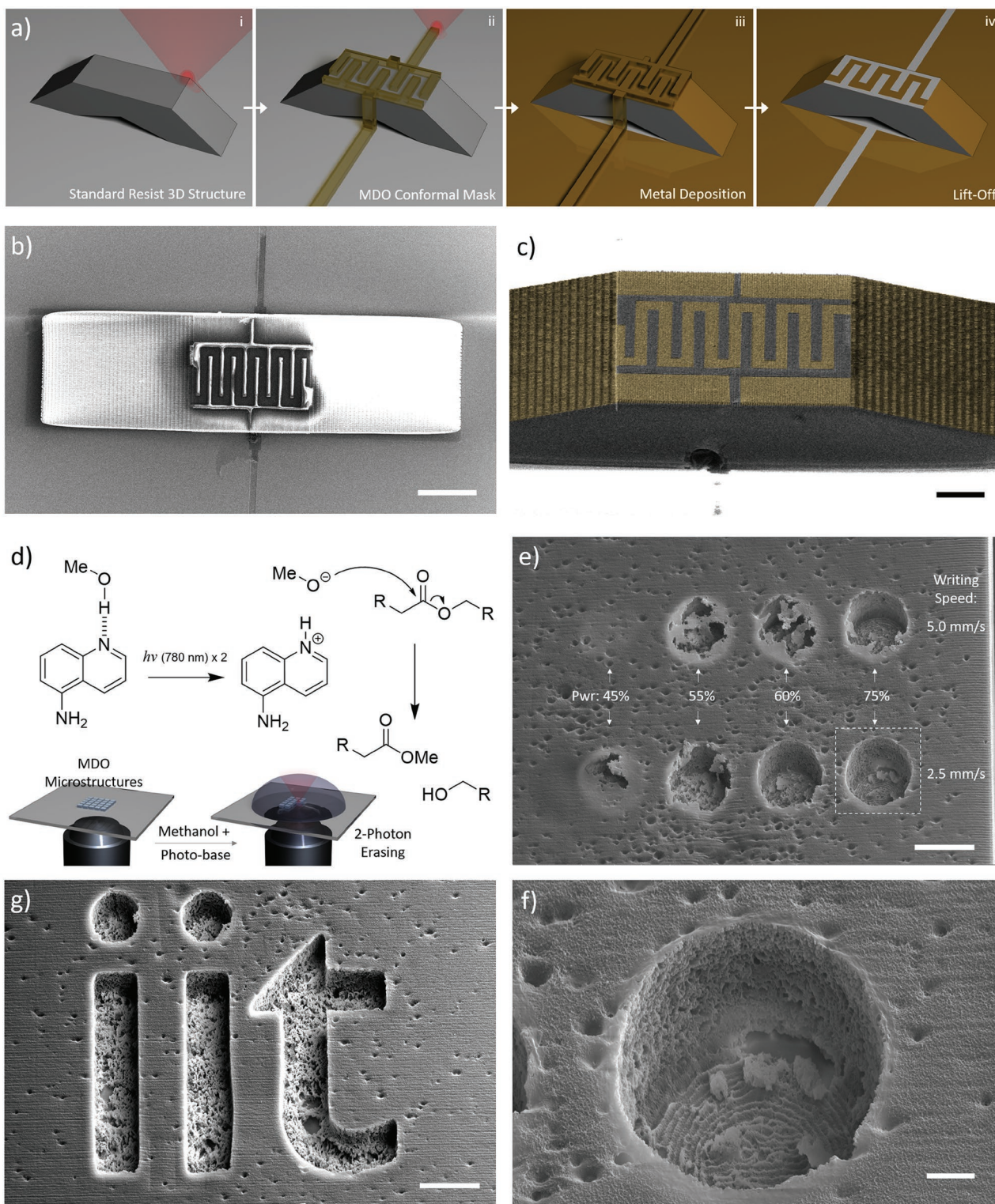


Figure 4. a) Schematic of a 3D masking methodology for the fabrication of an isolated serpentine on a DLW printed 3D structure: i) the main structure is printed through DLW; ii) an MDO formulation is employed to prepare a 3D sacrificial mask; iii) metal is evaporated on top; and iv) the mask is finally removed leaving a negative path on the structure. b) SEM pictures of the conductive serpentine obtained through the method described (employing MDO:IP-L 50:50 for the sacrificial mask) highlighting the non-conductive regions formed (scale bar 50 μm). c) False colors FIB image of the same structure (scale bar 20 μm). d) Mechanism of action of 4-AQ/MeOH mixture for the DLW-triggered degradation of aliphatic polyesters. e) SEM image of several DLW engraving tests of an MDO:IP-L 50:50 cube using a methanolic solution of 4-aminoquinoline employing different laser powers and writing speeds (scale bar 10 μm). f) Engraved IIT logo (scale bar 10 μm). g) Detail of an engraved cylinder using 75% laser power and 2.5 mm s^{-1} speed (scale bar 2 μm).

trait to a plethora of printed microstructures characterized by different functionalities and mechanical properties.

Finally, we show that it is also possible to trigger the degradation process locally employing a methanolic solution of a photobase that can be excited (to deprotonate methanol) in DLW conditions, thus achieving an even finer control over the subtractive performances of these formulations.

4. Experimental Section

Materials and Methods: 2-methylene-1,3-dioxepane (MDO, Fluorochem, United Kingdom), pentaerythritol tetraacrylate (PETA) with 1ppm inhibitor and 4-aminoquinoline (4AQ, TCI Chemicals, Japan), IP-L (Nanoscribe GmbH, Germany), poly(ethylene glycol) diacrylate average M_n 575 (PEG-DA), 3-[tris(trimethylsilyloxy)silyl]propyl methacrylate, trichloro(1H,1H,2H,2H-perfluorooctyl)silane, isopropyl alcohol (IPA), and Cyrene (SigmaAldrich, United Kingdom) were obtained by the aforementioned suppliers and used as received. Omnirad was kindly provided by IGM Resins B.V. (The Netherlands). IR-ATR spectra were recorded on a Shimadzu IRAffinit-1 spectrometer mounting a MIRacle 10 ATR module. Optical microscopy pictures were recorded on a Hirox KH-8700 digital microscope. SEM images were acquired with an EVO LS10 scanning electron microscope (Zeiss, Germany) at an accelerating voltage of 5 kV. FIB pictures and higher resolution SEM images were obtained with a Dual Beam FIB/SEM Helios Nano-Lab 600i (FEI), with at an accelerating voltage of 10 and 30 kV for electronic beam and ionic beam, respectively.

Printing via DLW: The calculated amount of photoinitiator, MDO, and crosslinker to prepare 200 mg of photoresist were mixed in a glass vial. (No photoinitiator was added in the case of MDO:IP-L mixtures.) The photoresist as prepared was transferred on a glass slide and placed in a Photonic Professional system (GT2) (Nanoscribe GmbH, Germany) which mounted 780 nm laser for the printing. In the case of formulations with low viscosity, the substrates were treated with 3-[tris(trimethylsilyloxy)silyl]propyl methacrylate (5 drops in 50 mL ethanol for a minimum of 2 h) or exposed to trichloro(1H,1H,2H,2H-perfluorooctyl)silane vapors for 1 h (while shading the printing region with Kapton tape). The authors perform the printing process using an oil immersion configuration, mounting a 63× lens. Hatching and slicing were set at 0.3 and 0.3 μm, respectively. A laser power of 4–20 mW (8% to 70% of the nominal 50 mW power at the lens, as indicated by the manufacturer) and writing speed from 1000 to 10 000 μm s⁻¹ were employed as described in the text. Development of the printed structures was performed by placing the substrates in IPA for 5 min. The unerasable part of the ‘donut’ in Figure 2 and the ‘bridge’ structure showed in Figure 4 were realized employing IP-L and IP-S as resists, respectively.

Decomposition Tests: The printed substrates comprising MDO were immersed (without stirring) in 50 mL of solutions of KOH in methanol (0.5–2 M), KOH in water (2.5 M), sulfuric acid in water (25 vol%), or AZ remover (1-aminopropan-2-ol) and heated to the desired temperature on a hotplate. The extent of the degradation was estimated by optical microscopy after rinsing the samples with either methanol or water followed by IPA and letting the solvent evaporate. A similar procedure was used in the case of the examples in Figures 3 and 4.

Etching with Photobase: A glass slide with printed structures on top, was placed in the printing setup as described in the previous paragraph and few drops of a freshly prepared 4-AQ solution in methanol (3.5 M) were added. The printing slot was then sealed to prevent methanol evaporation. Selective decomposition was performed using similar settings as the printing of MDO-comprising formulations, employing a laser power between 22.5–37.5 mW (45% and 70% of the nominal 50 mW power of the laser at the lens) and a laser speed between 2500 and 5000 μm s⁻¹. After the process, the structures were developed in IPA for 5 min.

Measurement of Mechanical Properties via Nanoindentation: On a glass slide, a series cylindrical pillars (height 60 μm, diameter 60 μm) were

printed employing IP-L (writing speed 10 mm s⁻¹; laser power 20 mW calculated as 40% of nominal 50 mW power at the lens), MDO:IP-L 3:1 (writing speed 10 mm s⁻¹; laser power 20 mW calculated as 40% of nominal 50 mW power at the lens), and MDO:IP-L 1:1 (writing speed 10 mm s⁻¹; laser power 35 mW calculated as 70% of nominal 50 mW power at the lens). A piece of Kapton tape (thickness 60 μm) was taped next to them for thickness reference and the mechanical properties measured using an Ultra Nanoindentation Tester (UNHT) (CSM Instruments, Switzerland), by using a cylindrical probe of 100 μm diameter, scanning speed of 30 μN s⁻¹, maximum load of 1000 μN (20 000 μN for yield stress evaluation), and a reference contact load of 500 μN. The linear parts of the forward stress–strain curves recorded were fitted in OriginPro 2018 (v. b9.5.1.195) to extract the Young modulus.

Supporting Information

Supporting Information is available from the Wiley Online Library or from the author.

Acknowledgements

The authors gratefully acknowledge Luca Ceseracciu and the Materials Characterization Facility at the Fondazione Istituto Italiano di Tecnologia for help with mechanical properties characterization of micro-samples. M.C. gratefully acknowledges support from the European Union’s Horizon 2020 research and innovation program under the Marie Skłodowska-Curie grant agreement MP3 – no. 885881. O.T. and V.M. gratefully acknowledge support from the European Union’s Horizon 2020 research and innovation program under the FET Open grant agreement 5DNanoPrinting – no. 899349.

Open access funding provided by Istituto Italiano di Tecnologia within the CRUI-CARE agreement.

Conflict of Interest

A patent application related to the presented work has been deposited at national (Italian) level in May 2021, by the same authors. Owner of the patent application is the Italian Institute of Technology.

Data Availability Statement

The data that support the findings of this study are available from the corresponding author upon reasonable request.

Received: December 7, 2021

Revised: February 26, 2022

Published online:

- [1] M. Carloti, V. Mattoli, *Small* **2019**, *15*, 1902687.
- [2] C. L. Lay, C. S. L. Koh, Y. H. Lee, G. C. Phan-Quang, H. Y. F. Sim, S. X. Leong, X. Han, I. Y. Phang, X. Y. Ling, *ACS Appl. Mater. Interfaces* **2020**, *12*, 10061.
- [3] S. K. Saha, D. Wang, V. H. Nguyen, Y. Chang, J. S. Oakdale, S.-C. Chen, *Science* **2019**, *366*, 105.
- [4] G. Seniutinas, A. Weber, C. Padeste, I. Sakellari, M. Farsari, C. David, *Microelectron. Eng.* **2018**, *191*, 25.
- [5] P. Kiefer, V. Hahn, M. Nardi, L. Yang, E. Blasco, C. Barner-Kowollik, M. Wegener, *Adv. Opt. Mater.* **2020**, *8*, 2000895.
- [6] O. Tricinci, M. Carloti, A. Desii, F. Meder, V. Mattoli, in *Adv. Fabr. Technol. Micro/Nano Opt. Photonics XIV* (Eds.: G. vonFreyermann, E. Blasco, D. Chanda), SPIE, Bellingham, WA **2021**, p. 17.

- [7] H. Wang, H. Wang, W. Zhang, J. K. W. Yang, *ACS Nano* **2020**, *14*, 10452.
- [8] O. Tricinci, T. Terencio, B. Mazzolai, N. M. Pugno, F. Greco, V. Mattoli, *ACS Appl. Mater. Interfaces* **2015**, *7*, 25560.
- [9] F. Mayer, S. Richter, P. Hübner, T. Jabbour, M. Wegener, *Adv. Mater. Technol.* **2017**, *2*, 1700212.
- [10] A. Marino, O. Tricinci, M. Battaglini, C. Filippeschi, V. Mattoli, E. Sinibaldi, G. Ciofani, *Small* **2018**, *14*, 1702959.
- [11] A. Marino, C. Filippeschi, V. Mattoli, B. Mazzolai, G. Ciofani, *Nanoscale* **2015**, *7*, 2841.
- [12] C. Barner-Kowollik, M. Bastmeyer, E. Blasco, G. Delaittre, P. Müller, B. Richter, M. Wegener, *Angew. Chem., Int. Ed.* **2017**, *56*, 15828.
- [13] H. Gehring, M. Blaicher, T. Grottko, W. H. P. Pernice, *IEEE J. Sel. Top. Quantum Electron.* **2020**, *26*, 1.
- [14] M. del Pozo, C. Delaney, C. W. M. Bastiaansen, D. Diamond, A. P. H. J. Schenning, L. Florea, *ACS Nano* **2020**, *14*, 9832.
- [15] M. Hippler, E. Blasco, J. Qu, M. Tanaka, C. Barner-Kowollik, M. Wegener, M. Bastmeyer, *Nat. Commun.* **2019**, *10*, 232.
- [16] C. Delaney, J. Qian, X. Zhang, R. Potyrailo, A. L. Bradley, L. Florea, *J. Mater. Chem. C* **2021**, *9*, 11674.
- [17] M. Restaino, N. Eckman, A. T. Alsharhan, A. C. Lamont, J. Anderson, D. Weinstein, A. Hall, R. D. Sochol, *Adv. Mater. Technol.* **2021**, *6*, 2100222.
- [18] T. Baghdasaryan, K. Vanmol, H. Thienpont, F. Berghmans, T. Geernaert, J. Van Erps, *J. Phys.: Photonics* **2021**, *3*, 045001.
- [19] M. Belqat, X. Wu, L. P. C. Gomez, J.-P. Malval, S. Dominici, B. Leuschel, A. Spangenberg, K. Mougouin, *Addit. Manuf.* **2021**, *47*, 102232.
- [20] A. Münchinger, V. Hahn, D. Beutel, S. Woska, J. Monti, C. Rockstuhl, E. Blasco, M. Wegener, *Adv. Mater. Technol.* **2021**, *7*, 2100944.
- [21] M. Carlotti, O. Tricinci, F. den Hoed, S. Palagi, V. Mattoli, *Open Res. Eur.* **2021**, *1*, 129.
- [22] C. A. Spiegel, M. Hackner, V. P. Bothe, J. P. Spatz, E. Blasco, *Adv. Funct. Mater.* **2022**, 2110580.
- [23] A. J. Gross, K. Bertoldi, *Small* **2019**, *15*, 1902370.
- [24] B. J. Adzima, C. J. Kloxin, C. A. DeForest, K. S. Anseth, C. N. Bowman, *Macromol. Rapid Commun.* **2012**, *33*, 2092.
- [25] D. Gräfe, S. L. Walden, J. Blinco, M. Wegener, E. Blasco, C. Barner-Kowollik, *Angew. Chem., Int. Ed.* **2020**, *59*, 6330.
- [26] M. M. Zieger, P. Mueller, A. S. Quick, M. Wegener, C. Barner-Kowollik, *Angew. Chem., Int. Ed.* **2017**, *56*, 5625.
- [27] M. M. Zieger, P. Müller, E. Blasco, C. Petit, V. Hahn, L. Michalek, H. Mutlu, M. Wegener, C. Barner-Kowollik, *Adv. Funct. Mater.* **2018**, *28*, 1801405.
- [28] R. Batchelor, T. Messer, M. Hippler, M. Wegener, C. Barner-Kowollik, E. Blasco, *Adv. Mater.* **2019**, *31*, 1904085.
- [29] H. A. Houck, P. Müller, M. Wegener, C. Barner-Kowollik, F. E. Du Prez, E. Blasco, *Adv. Mater.* **2020**, *32*, 2003060.
- [30] D. Gräfe, M. Gernhardt, J. Ren, E. Blasco, M. Wegener, M. A. Woodruff, C. Barner-Kowollik, *Adv. Funct. Mater.* **2020**, *31*, 2006998.
- [31] S. Agarwal, C. Speyerer, *Polymer* **2010**, *51*, 1024.
- [32] W. J. Bailey, Z. Ni, S. R. Wu, *Macromolecules* **1982**, *15*, 711.
- [33] S. Agarwal, *Polym. Chem.* **2010**, *1*, 953.
- [34] J. Folini, W. Murad, F. Mehner, W. Meier, J. Gaitzsch, *Eur. Polym. J.* **2020**, *134*, 109851.
- [35] C. A. Bell, G. G. Hedir, R. K. O'Reilly, A. P. Dove, *Polym. Chem.* **2015**, *6*, 7447.
- [36] S. Agarwal, *Polym. J.* **2007**, *39*, 163.
- [37] G. G. Hedir, C. A. Bell, R. K. O'Reilly, A. P. Dove, *Biomacromolecules* **2015**, *16*, 2049.
- [38] S. Komatsu, T. A. Asoh, R. Ishihara, A. Kikuchi, *Polymer* **2019**, *179*, 121633.
- [39] P. Xu, X. Huang, X. Pan, N. Li, J. Zhu, X. Zhu, *Polymers* **2019**, *11*, 318.
- [40] T. Cai, Y. Chen, Y. Wang, H. Wang, X. Liu, Q. Jin, S. Agarwal, J. Ji, *Polym. Chem.* **2014**, *5*, 4061.
- [41] G. Dai, Q. Xie, C. Ma, G. Zhang, *ACS Appl. Mater. Interfaces* **2019**, *11*, 11947.
- [42] D. Ding, X. Pan, Z. Zhang, N. Li, J. Zhu, X. Zhu, *Polym. Chem.* **2016**, *7*, 5258.
- [43] A. W. Jackson, L. R. Chennamaneni, S. R. Mothe, P. Thoniyot, *Chem. Commun.* **2020**, 56, 9838.
- [44] A. Tardy, J. Nicolas, D. Gigmes, C. Lefay, Y. Guillauneuf, *Chem. Rev.* **2017**, *117*, 1319.
- [45] S. Reddy Mothe, J. S. J. Tan, L. R. Chennamaneni, F. Aidil, Y. Su, H. C. Kang, F. C. H. Lim, P. Thoniyot, *J. Polym. Sci.* **2020**, *58*, 1728.
- [46] A. Tardy, N. Gil, C. M. Plummer, D. Siri, D. Gigmes, C. Lefay, Y. Guillauneuf, *Angew. Chem.* **2020**, *132*, 14625.
- [47] A. Tardy, J.-C. Honoré, J. Tran, D. Siri, V. Delplace, I. Bataille, D. Letourneur, J. Perrier, C. Nicoletti, M. Maresca, C. Lefay, D. Gigmes, J. Nicolas, Y. Guillauneuf, *Angew. Chem.* **2017**, *129*, 16742.
- [48] A. Tardy, N. Gil, C. M. Plummer, C. Zhu, S. Harrisson, D. Siri, J. Nicolas, D. Gigmes, Y. Guillauneuf, C. Lefay, *Polym. Chem.* **2020**, *11*, 7159.
- [49] S. F. Alamudun, K. Tanovitz, A. Fajardo, K. Johnson, A. Pham, T. Jamshidi Araghi, A. S. Petit, *J. Phys. Chem. A* **2020**, *124*, 2537.
- [50] E. W. Driscoll, J. R. Hunt, J. M. Dawlaty, *J. Phys. Chem. A* **2017**, *121*, 7099.
- [51] J. R. Hunt, J. M. Dawlaty, *J. Phys. Chem. A* **2018**, *122*, 7931.